

Research article

Prediction of creep behavior of Wengé (*Millettia Laurentii*) by the discrete Kalman filter based on Burger's rheological model

*PriscaKuida Atchounga¹, Emmanuel Foadieng² and Pierre KisitoTalla¹

University of Dschang¹ and University of Buéa²
Mechanics and Modeling of Physical Systems Research Unit (*UR-2MSP*)
Dschang, Cameroon

*Correspondence: patchoungakuida@yahoo.com



This work is licensed under a [Creative Commons Attribution 4.0 International License](https://creativecommons.org/licenses/by/4.0/)

Abstract

The purpose of this research work is the modeling of creep behavior of the wood species « *Millettia Laurentii* » via a probabilistic method that is the kalman filter. In the first part of this work, the theory on the Kalman filter is presented and it is followed by the presentation of the Burger's rheological model that allows us to determine the dynamic model of the filter. Physical and mechanical properties of this hardwood are determined; then we attempt to model the creep behavior of wood for the first time using discrete Kalman filter. After modeling our system, we try to predict creep with this filter under MATLAB software. It came out that the strain exponentially increased during primary creep while the shape during secondary creep was linear. These results showed that Kalman estimate were up to various theories on creep; we also proved that the filter converges because the estimation error was minimal. Consequently, Kalman filter constitutes a powerful optimal predictor which can be applied in the field of rheology to follow up the creep behavior of polymeric materials. Our model has been validated by the means of Burger model from which we established the dynamic model of the filter. **Copyright © WJSTR, all rights reserved.**

Keywords: Kalman filter, Millettia Laurentii, Creep, Stress, Burger rheological model.

1 Introduction

During the last few years, much attention has been paid to the application of wood in various engineering works in the world. Due to the expensiveness of traditional materials like steel, iron, concrete, etc.,

wood has become a world-wide alternative[1- 4]. Meanwhile creep is among the fundamental factors limiting its long-term application as excessive deformation or reduced stiffness occurs over an extended period of time. For material design related to the load-bearing capacity of products, the evaluation of creep behavior is indispensable[5-6].

Rheological models used to describe the creep behavior of wood in the literature are classic methods that do not have an imprecision term that can allow correct estimations in spite of modeling errors. This constitutes a major problem to the science of materials. We then thought that the Kalman filter can be a solution to this preoccupation.

2 Theory on Kalman filter

In 1960 Kalman published his paper describing a recursive solution to the discrete-data linear filtering problem [7]. Since that time, due in large part to advances in digital computing; the Kalman filter has been the subject of extensive research and application, particularly in the area of autonomous or assisted navigation[8-9].

2.1 The process to be estimated

The Kalman filter addresses the general problem of trying to estimate the state x of a discrete-time controlled process that is governed by the linear stochastic difference equation

$$x_{k+1} = Ax_k + Bu_k + w_k \quad (1)$$

With a measurement equation

$$y_k = Hx_k + v_k \quad (2)$$

The random variables w_k and v_k represent the process and measurement noises respectively. They are assumed to be independent of each other, white and with normal probability distributions [10]. A white noise is a stochastic process with autocorrelation different from zero only at the origin but zero everywhere. It is a de-correlated process.

$$p(w) = N(0, Q) \text{ and } p(v) = N(0, R) \text{ with } Q = E[w_k w_k^T] \text{ and } R = E[v_k v_k^T] \quad (3)$$

Here, we assume constant the *process noise covariance* Q and *measurement noise covariance* R matrices.

In the above equations A , B and H are constant matrices, k is the time index; x is called the state of the system; u is a known input to the system and y is the measured output vector. The vector x contains all of the information about the present state of the system, but we cannot measure x directly. Instead we measure y , which is a function of x that is corrupted by the noise v . We can use y to help us obtain an estimate of x , but we cannot necessarily take the information from y at face value because it is corrupted by noise.

2.2 The computational origins of the filter

We define \hat{x}_k^- to be our a priori state estimate at step k given knowledge of the process prior to step k , and \hat{x}_k^+ to be our a posteriori state estimate at step k given measurement y_k . We can define a priori and a posteriori estimate errors as

$$e_k^- = x_k - \hat{x}_k^- \text{ and } e_k^+ = x_k - \hat{x}_k^+ \quad (4)$$

The a priori estimate error covariance is then

$$P_k^- = E[e_k^- e_k^{-T}] \quad (5)$$

And the a posteriori estimate error covariance is

$$P_k^+ = E[e_k^+ e_k^{+T}] \quad (6)$$

In deriving the equations for the Kalman filter, we begin with the goal of finding an equation that computes an a posteriori state estimate x_k^+ as a linear combination of an a priori estimate x_k^- and a weighted difference between an actual measurement y_k and a measurement prediction Hx_k^- as shown below (7)

$$x_k^+ = x_k^- + K(y_k - Hx_k^-) \quad (7)$$

The difference $(y_k - Hx_k^-)$ is called the measurement innovation, or the residual. The matrix K in (7) is chosen to be the Kalman gain that minimizes the a posteriori error covariance (6). One popular form of the resulting K that minimizes (6) is given by [11]

$$K_k = P_k^- H^T (HP_k^- H^T + R)^{-1} \quad (8)$$

2.2 The Kalman algorithm

The Kalman filter estimates a process by using a form of feedback control: the filter estimates the process state at some time and then obtains feedback in the form of noisy measurements. As such, the equations for the Kalman filter fall into two groups: time update equations also called predictor equations and measurement update equations referred to as corrector equations. The predictor equations are responsible for projecting forward the current state and error covariance estimates to obtain the a priori estimates for next time step. The corrector equations are responsible for the feedback[12-13].

The specific equations for the prediction step are the following:

$$x_{k+1}^- = Ax_k + Bu_k \quad (9)$$

$$P_{k+1}^- = AP_k A^T + Q \quad (10)$$

The specific corrector equations are the following:

$$K_{k+1} = P_{k+1}^- H^T (HP_{k+1}^- H^T + R)^{-1} \quad (11)$$

$$x_{k+1}^+ = x_{k+1}^- + K_{k+1} (y_k - Hx_{k+1}^-) \quad (12)$$

$$P_{k+1}^+ = P_{k+1}^- - K_{k+1} H P_{k+1}^- \quad (13)$$

3 Prediction of creep behavior by the means of Kalman filter

3.1 Derivation of the differential equation of the Burger's rheological model

Let's consider a wood tube undergoing a constant stress σ on the test machine (figure 1). Due to this load, the wood tube undergoes deformation as time is passing and constitutes a dynamic system. We have chosen the Burger's rheological model to establish the differential equation that describes the temporal evolution of our system.

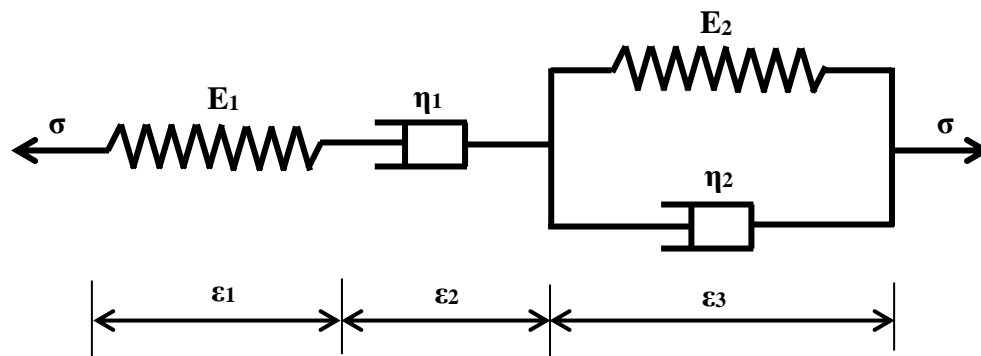


Figure 1 : Fourthorder Burger's rheological model

From this figure it follows that:

$$\sigma = E_1 \varepsilon_1, \sigma = \eta_1 \dot{\varepsilon}_2, \sigma = E_2 \varepsilon_3 + \eta_2 \dot{\varepsilon}_3 \quad (14a-c)$$

Where σ is the applied stress, $\varepsilon_1, \varepsilon_2, \varepsilon_3$ are respectively the strains in the spring of Young modulus E_1 , the dashpot of viscosity η_1 and the spring of Young modulus E_2 . Still from the preceding figure, the total strain due to the stress σ is given by:

$$\varepsilon = \varepsilon_1 + \varepsilon_2 + \varepsilon_3 \quad (15)$$

From the equation (15) it comes that

$$\dot{\varepsilon}_1 = \dot{\varepsilon} - \dot{\varepsilon}_2 - \dot{\varepsilon}_3 \quad (16)$$

Where the dot “.” stands for the first derivative relative to time.

Combining equations (14a-c) and (16), leads to

$$\frac{\dot{\sigma}}{E_1} = \dot{\varepsilon} - \left(\frac{1}{\eta_1} + \frac{1}{\eta_2} \right) \sigma + \frac{E_2 \varepsilon_3}{\eta_2} \quad (17)$$

Substituting equations (14a) and (15) into (17) gives

$$\frac{\dot{\sigma}}{E_1} = \dot{\varepsilon} - \left(\frac{1}{\eta_1} + \frac{1}{\eta_2} \right) \sigma + \frac{E_2}{\eta_2} \left(\varepsilon - \frac{\sigma}{E_1} - \varepsilon_2 \right) \quad (18)$$

Let's derive equation (18) and insert into equation (14b), we obtain

$$\frac{\ddot{\sigma}}{E_1} = \ddot{\varepsilon} - \left(\frac{1}{\eta_1} + \frac{1}{\eta_2} \right) \dot{\sigma} + \frac{E_2}{\eta_2} \dot{\varepsilon} - \frac{E_2}{\eta_2 E_1} \dot{\sigma} - \frac{E_2}{\eta_2 \eta_1} \sigma \quad (19)$$

where the double dot “.” represents the second derivative with respect to time. The equation (19) can be rewritten as follows :

$$\frac{\eta_1 \eta_2}{E_1 E_2} \ddot{\sigma} + \left[\frac{\eta_2}{E_2} + \eta_1 \left(\frac{1}{E_1} + \frac{1}{E_2} \right) \right] \dot{\sigma} + \sigma = \eta_1 \dot{\varepsilon} + \frac{\eta_1 \eta_2}{E_2} \ddot{\varepsilon} \quad (20)$$

The equation (20) is a second order inhomogeneous partial differential ordinary equation. The time “t” is the independent variable, and the unknown function is the stress $\sigma(t)$, that depends also on the strain $\varepsilon(t)$.

3.2 Derivation of the Kalman filter components

Since our target is the evolution of the strain $\varepsilon(t)$ for a given constant applied stress ($\sigma = \sigma_0 = \text{constant}$), then we should have $\dot{\sigma} = \ddot{\sigma} = 0$. The preceding equation (20) becomes:

$$\frac{\eta_1 \eta_2}{E_2} \ddot{\varepsilon}(t) + \eta_1 \dot{\varepsilon}(t) = \sigma_0 \quad (21)$$

We should mention here that our main contribution in the modeling of wood creep behavior relies on the introduction of an uncertainty term in the equation (21), in order to obtain a new relation capable of predicting the strain of a material. This prediction is followed automatically by the correction of the gauge noise and the modeling errors.

In this equation, $\dot{\varepsilon}(t)$ and $\ddot{\varepsilon}(t)$ stand for the strain rate and the strain acceleration. Let us rewrite equation (21) in the form of the process equation, the two previous derivatives become:

$$\ddot{\varepsilon}(t) = \frac{\dot{\varepsilon}(t) - \dot{\varepsilon}(t - \Delta t)}{\Delta t} \text{ avec } \dot{\varepsilon}(t) = \frac{\varepsilon(t) - \varepsilon(t - \Delta t)}{\Delta t} \quad (22)$$

Substituting equation (22) into (21) leads us to

$$\varepsilon(t) = \varepsilon(t - \Delta t) + \frac{\Delta t}{1 + \frac{E_2 \Delta t}{\eta_2}} \dot{\varepsilon}(t - \Delta t) + \frac{\Delta t^2}{1 + \frac{E_2 \Delta t}{\eta_2}} \alpha \quad (23)$$

$$\text{with } \alpha = \frac{E_2 \sigma_0}{\eta_1 \eta_2} \quad (24)$$

We also the following equation (25) in complement with equation (23)

$$\dot{\varepsilon}(t) = \dot{\varepsilon}(t - \Delta t) + \alpha \Delta t \quad (25)$$

The term α is homogenous to strain acceleration of the wood tube under constant stress σ_0 . We should discretize equations (23) and (25) in times of time index k , with the means of the relation $t = k \cdot \Delta t$ [14]. So we have the following relation :

$$\begin{cases} \varepsilon(t) = \varepsilon(k \Delta t) = \varepsilon_k \\ \varepsilon(t - \Delta t) = \varepsilon(k \Delta t - \Delta t) = \varepsilon[(k - 1) \Delta t] = \varepsilon_{k-1} \end{cases} \quad (26)$$

Equations (23) and (25) can be rewritten in the following form

$$\begin{pmatrix} \varepsilon_{k+1} \\ \dot{\varepsilon}_{k+1} \end{pmatrix} = \begin{bmatrix} 1 & \frac{\Delta t}{1 + \frac{E_2 \Delta t}{\eta_2}} \\ 0 & 1 \end{bmatrix} \begin{pmatrix} \varepsilon_k \\ \dot{\varepsilon}_k \end{pmatrix} + \begin{bmatrix} \frac{\Delta t^2}{1 + \frac{E_2 \Delta t}{\eta_2}} \\ \Delta t \end{bmatrix} \alpha + w_k \quad (27)$$

Let $x_k \begin{pmatrix} \varepsilon_k \\ \dot{\varepsilon}_k \end{pmatrix}$ and $x_{k+1} \begin{pmatrix} \varepsilon_{k+1} \\ \dot{\varepsilon}_{k+1} \end{pmatrix}$ be respectively the state vectors at the given dates k et $k+1$, then the equation (27) can take the following form :

$$x_{k+1} = Ax_k + Bu_k + w_k \quad (28)$$

where the matrices A and B are identified from equation (27). Here w_k stands for the process noise due for example to modeling errors, to irregularities and wood defects. The control parameter of our system is $u_k = \alpha$.

Since the dynamic model of our system is known (equation 28), we should now find the measurement equation which is the second equation of the Kalman filter.

In the laboratory we are dealing with sensors (strain gauges and extensometer) that allow us to measure the wood strain ε_k , then our measurement matrix H would be a line vector with both the two elements equal to one. Our measurement vector y_k would have two elements at any date. At time k our measurement equation has the form :

$$y_k = [1 \quad 1] x_k + v_k \quad (29)$$

In equation (29), v_k stands for the noise measurement generated by the sensors (extensometer and strain gauges) and its covariance matrix is $R(t_k)$.

Our purpose is to estimate at any date t_k the strain ε_k and the strain rate $\dot{\varepsilon}_k$. Of course the state vector x_k has two components all the time :

$$x_k = \begin{pmatrix} \varepsilon_k \\ \dot{\varepsilon}_k \end{pmatrix} \quad (30)$$

Since we need the previous state vector as our initial guess to compute the a priori actual state, we should set the values of the state vector at the initial date t_0 . For a wood tube lying initially on the test machine and not yet undergoing the stress σ , we should set that its a priori strain at $t_0 = 0^-$ is zero that is $\varepsilon_0^- = 0$; in a similar manner its strain rate at the same date would be zero $\dot{\varepsilon}_0^- = 0$. The a posteriori strain of the wood tube ε_0^+ refers to its initial instantaneous strain at the date $t_0 = 0^+$ of application of the stress σ . So at any time the a priori value x_k^- and the a posteriori value x_k^+ are both the two components of the state vector. The initial guess is the following state vector :

$$x_0^+ = \begin{pmatrix} \varepsilon_0^+ \\ \dot{\varepsilon}_0^+ \end{pmatrix} \quad (31)$$

The values of the state vector at the future dates t_1, t_2, \dots, t_n would be estimated by the means of this initial guess.

We should now find the value of the covariance matrix of initial estimation P_0 , in order to correct the uncertainty that corrupts our initial guess. This initial covariance matrix is a second order diagonal squared matrix with elements representing respectively the standard deviation on the strain and on the strain rate.

$$P_0 = \begin{bmatrix} \xi(\varepsilon) & 0 \\ 0 & \xi(\dot{\varepsilon}) \end{bmatrix} \quad (32)$$

The covariance matrices of dynamic noise Q and of measurement noise R are diagonal matrices with elements representing respectively variances on strain and on strain rate. These matrices are given by the following formula :

$$Q = E(w_k \cdot w_k^T) = \begin{bmatrix} \xi_1^2(\varepsilon) & 0 \\ 0 & \xi_1^2(\dot{\varepsilon}) \end{bmatrix} \quad (33)$$

$$R = E(v_k \cdot v_k^T) = \begin{bmatrix} \xi_2^2(\varepsilon) & 0 \\ 0 & \xi_2^2(\dot{\varepsilon}) \end{bmatrix} \quad (34)$$

Here "E" stands for the mean of the considered quantity.

4 Experimental setup

The material tested here is the wood called vernacularly “Wengé” and its botanic name is “*Millettia Laurentii*”. We carried out the experiments on three samples well dried of this Cameroonian wood species. The selected samples did not have any macroscopically observable defect. They were all rectangular and had 34 cm of length, 2 cm of width and 2 cm of thickness. The strain was measured using $R = 120\Omega \pm 0.3\%$ strain gauges connected in an half Wheatstone bridge as indicated in Figure 2. On every specimen was fixed symmetrically two strain gauges. The strain was converted into deformation using the strain bridge EI 616 from DELTALAB. The creep lasted for 10 hours and the recovery for 40 hours.

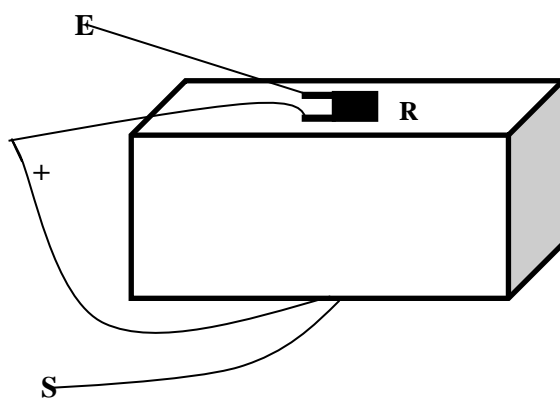


Figure 2 . Wood tube carrying two symmetrical gauges

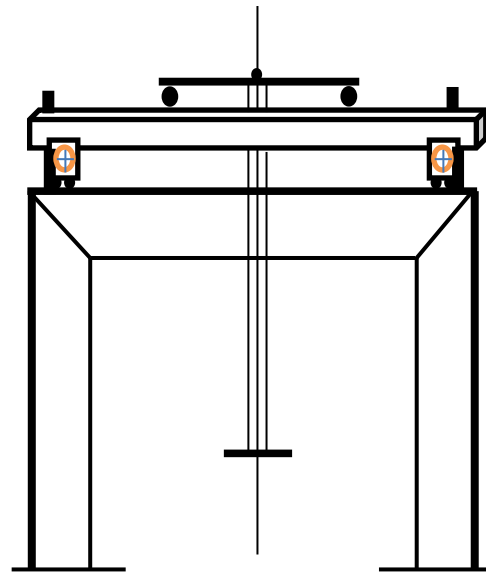


Figure 3. Bending creep testing device

On this figure 2, E and S represent the gauge electrodes that are directly connected to the strain bridge and R stands for the gauge electrical resistance. During the test the sample is laid on the test machine in such a way that one gauge is on the top and another one symmetrically on the opposite face of the sample.

The device used for the bending creep test is illustrated by the diagram in Figure 3. The device setup was inside the air-condition room. Each specimen was placed horizontally on the two supporting points of the device. The distance between the supporting points was 340 mm. A symmetrical load was applied at each of the third-points of the specimen. At the supporting points and at the loading points, we used a cylinder made of steel, to press the surfaces of the beam, in order to minimize the perpendicular shearing strain. We tested all the three samples with six different loads.

5 Result and discussion

5.1 Physical and mechanical properties of *Millettia Laurentii*

The moisture content of all the wood tubes were **12%**, at this value the relative density was $\rho = 0,790 \text{ g/cm}^3$. This wood species has a fiber saturated point of **23%**, its Young modulus in longitudinal direction is $E_L = 21058 \text{ MPa}$. Still in the longitudinal direction, the average breaking stress in compression test was $\sigma_{c/moy} = 78,5 \text{ MPa}$ and its average breaking stress (ABS) perpendicularly to fibers in flexural test was $\sigma_{FLmoy} = 154,6 \text{ MPa}$. We should mention here that these properties have been determined following the French Norm NF B 51-003 that labels general requirements for physical and mechanical tests.

5.2 Determination of the Burger's parameters

At this level as we mentioned before, the tests was carried out on three samples of Wengé wood that we named respectively W_1 , W_2 and W_3 . Every sample has been tested in flexural test under six levels of stress ranging from **10,70% ABS** to **27,83% ABS**. During creep test, every sample undergoes the applied stress for a time period of 10 hours and followed by 40 hours of recovery. Then the experimental values obtained during creep test were exploited to determine the four burger's parameters. We should mention here that these parameters have been determined through a convergent optimization procedure under MATLAB software[15].

Table1. Burger's parameters of specimen W_1

σ (MPa)	E_1 (10^4 MPa)	E_2 (10^5 MPa)	η_1 (10^8 MPa.min)	η_2 (10^6 MPa.min)	τ (min)
10,70% ABS	3,29	7,7	2,8	13,3	17,31
18,19% ABS	1,23	2,70	2,6	5,8	21
21,41% ABS	1,1	1,5	2,0	3,5	23,33
24,62% ABS	0,805	2,9	1,6	5,1	17,58
27,83% ABS	0,833	2,69	2,2	4,5	17,03

Table2. Burger's parameters of specimen W_2

σ (MPa)	E_1 (10^4 MPa)	E_2 (10^5 MPa)	η_1 (10^8 MPa.min)	η_2 (10^6 MPa.min)	τ (min)
10,70% ABS	1,57	2,85	3,0	5,9	20,76
14,98% ABS	1,05	3,5	5,2	11,8	33,80
18,19% ABS	0,932	2,48	2,5	4,1	16,8
21,41% ABS	0,84	2,61	1,9	5,2	19,98
24,61% ABS	0,805	2,62	2,2	7,8	36,32
27,83% ABS	0,833	2,63	2,6	4,6	17,55

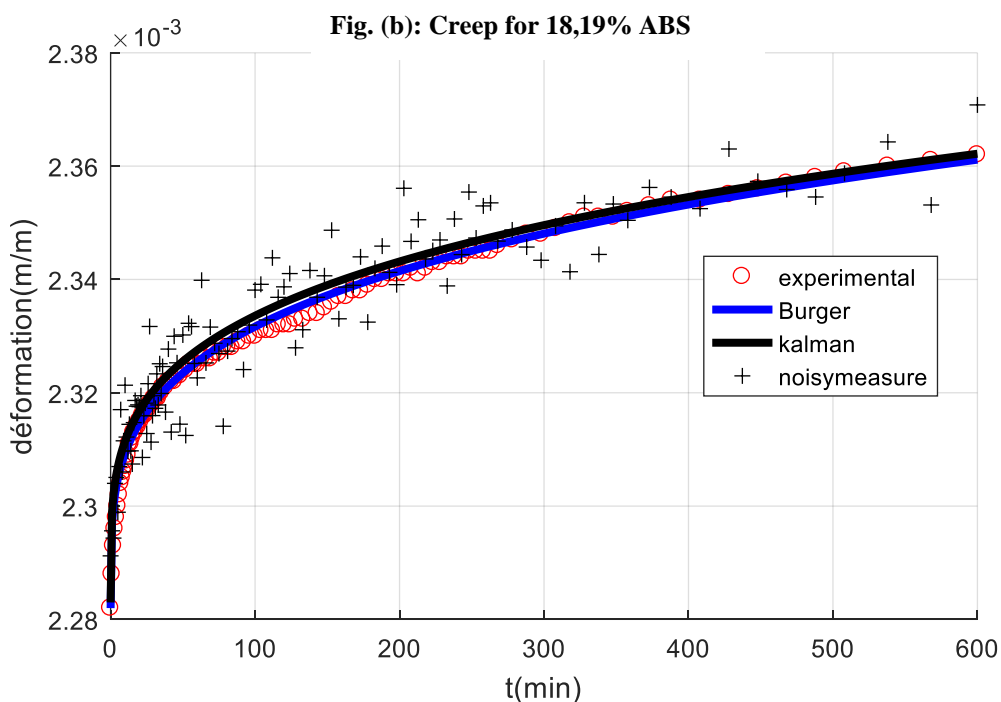
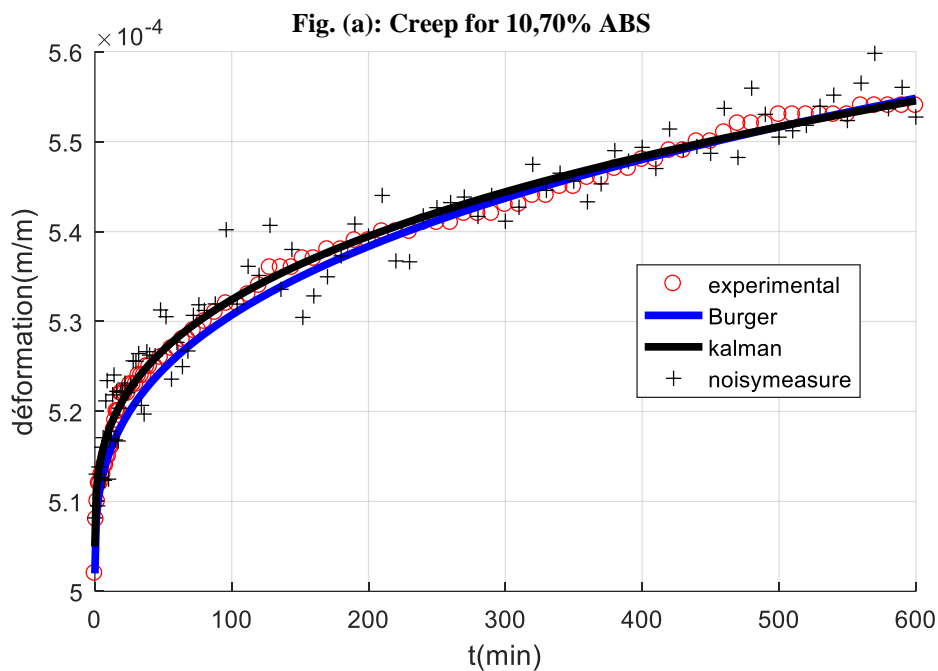
Table 3. Burger's parameters of specimen W_3

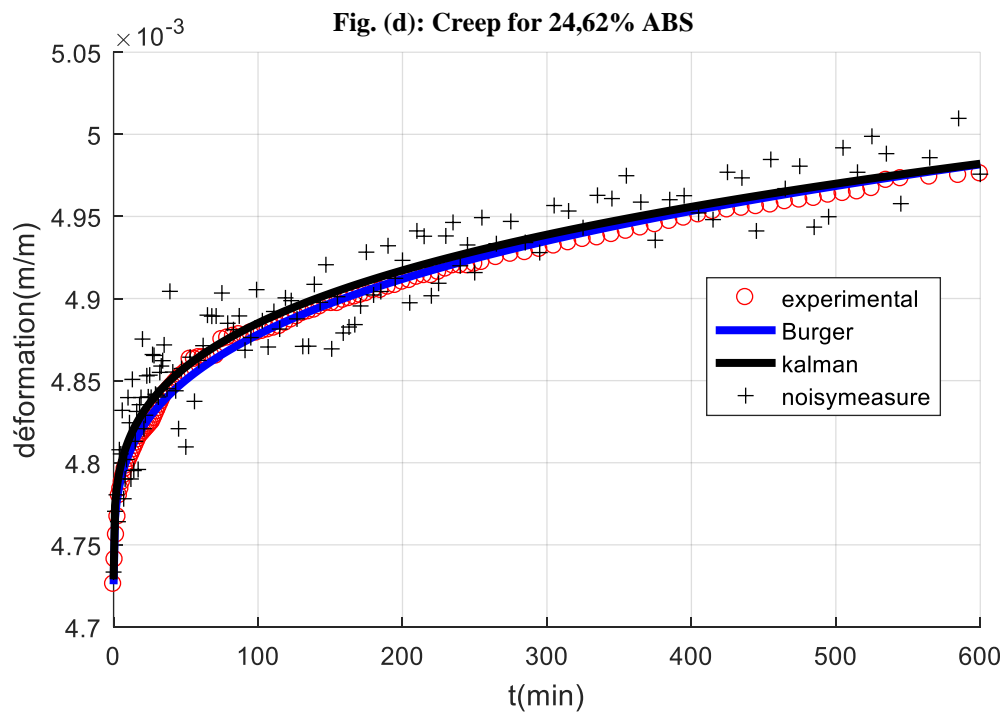
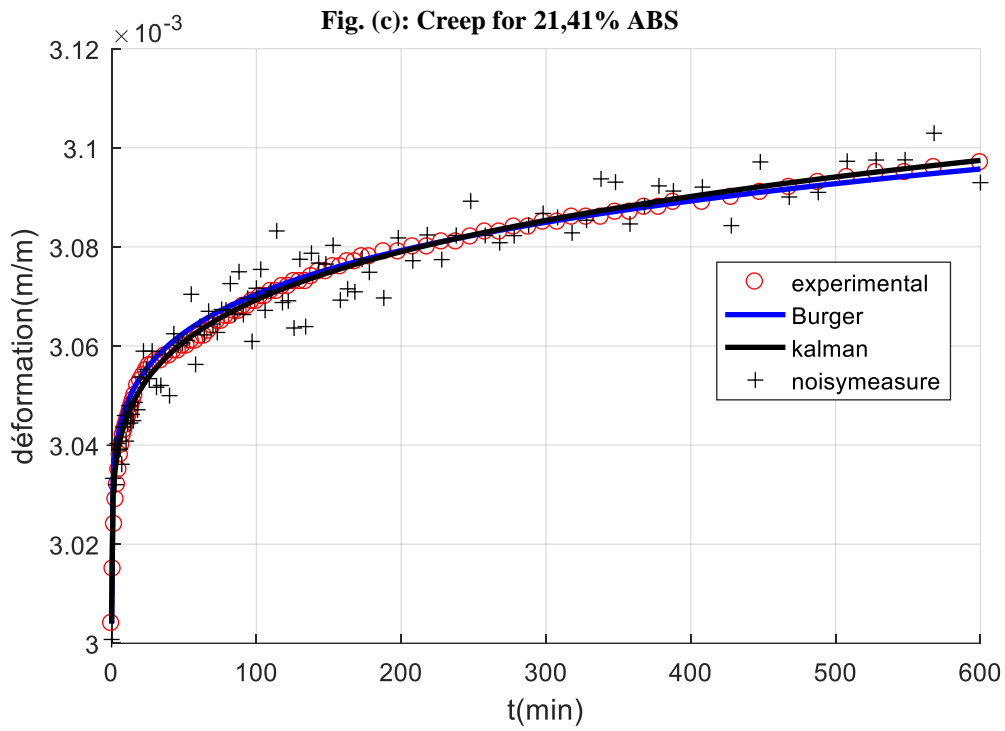
σ (MPa)	E_1 (10^4 MPa)	E_2 (10^5 MPa)	η_1 (10^8 MPa.min)	η_2 (10^6 MPa.min)	τ (min)
10,70% ABS	1,83	3,07	3,33	8,86	28,88
14,98% ABS	1,2	3,1	2,76	8,88	28,65
18,19% ABS	1	3,7	3,4	12,5	33,78
21,41% ABS	0,936	3,3	3,7	16,66	50,50
24,61% ABS	0,874	3,5	2,91	83,33	23,80

We can underline here that these parameters have been used to determine the retardation time of every wood sample. This retardation time (τ) is often interpreted as the time needed by the test specimen to deform to 63,21% ($\equiv [1 - e^{-1}]$ %) of the total deformation[16]. Polymeric viscoelastic materials have a large number of characteristic retardation times distributed over many decades [17]. It is good to know that on these tables, we didn't present the results at the stress levels where the materials didn't response well.

5.3 Presentation of creep curves

After determining all the parameters of the Kalman filter, we can now appreciate how this predictor tool works. So the deformation (strain) is measured with a standard deviation of 10^{-3} m/m corresponding to a variance of 10^{-6} m²/m² and the strain rate with a standard deviation of 10^{-2} m/m/s corresponding to a variance of 10^{-4} m²/m²/s². But in the following section we will just present strain curves which is the most relevant parameter of the tested specimen. Only the creep curves of specimen W1 are showed here because the other two specimens had almost the same curves. Now we have introduced all the mentioned parameters in the Kalman loop and the results obtained are the following:





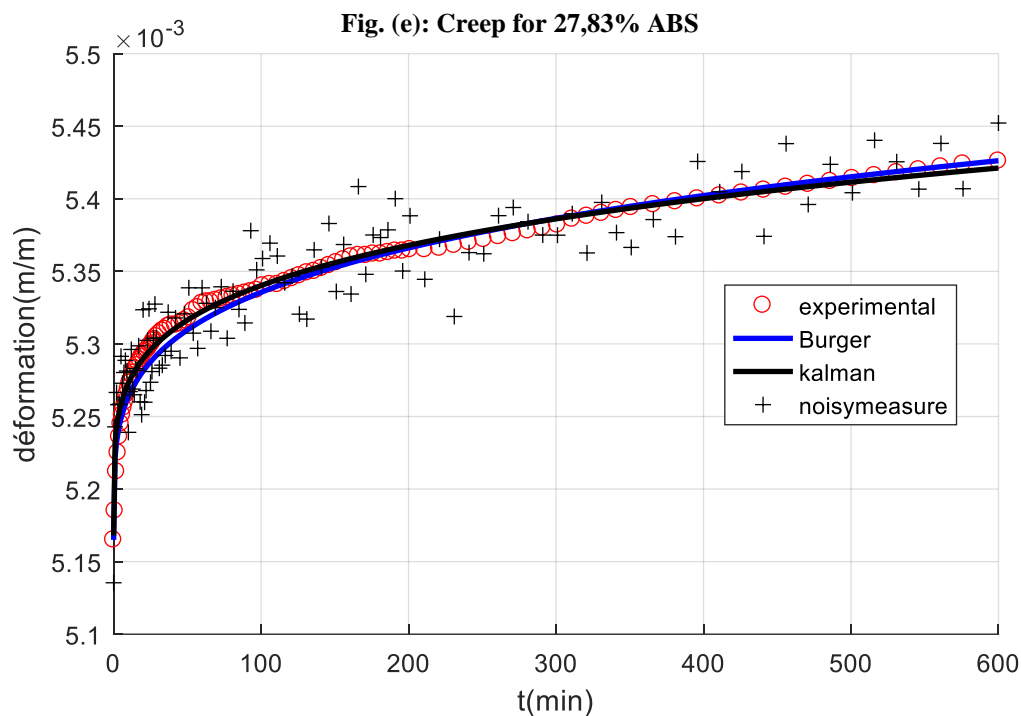


Figure 4. Creep curves of specimen W1 : the Burger curve is in blue, the experimental curve is in red, the Kalman prediction is in black and the noisy strain curve is the black crosses.

From the preceding figures, it is obvious that Kalman predictions based on Burger model fit well the experimental values of creep. Only primary and secondary creeps are represented here because we tested our samples under low stress levels compared to the average breaking stress. We made this choice because one of the characteristics of the Burger rheological model is that it works well under low stress. Moreover by scrutinizing these figures, it comes that Kalman estimates are smoother than the noisy measurements. Since the Kalman predictions and the experimental values are so closed each to other that it is difficult to distinguish them, it just certifies that the filter converges. We should bear in mind that the the various matrices presented in the filter changes values with the applied stress on the specimen. Several research works have been devoted to the creep behavior of polymeric materials [18-21]. The main advantage that offers the Kalman filter is that; once the initial value of the deformation is known the deformations at future dates can be estimated with a good precision by minimizing the estimation error [22].

The primary creep stretches on a reduced time interval (that is between 0 and 100 minutes) where reigns severe test conditions. It is an accommodation phase of the material to the stress; characterized by the decrement of the strain rate. It corresponds to a reorganization of the material (alignment of chain rings, orientation of macromolecular structure) consecutive to the application of the stress. The secondary stage or phase of the stabilization of deformation is the most extended zone (beyond 100 minutes), it is characterized by a constant and minimal strain rate and is a stability phase.

It comes from these figures that the estimation error is minimal, due to the fact that the Kalman filter has minimized the variance of the estimation error. On this point of view, the Kalman filter is an optimal

predictor. The following figures are the characteristics of the noise that perturbs the deformation of the material. It is evident that it is a white noise.

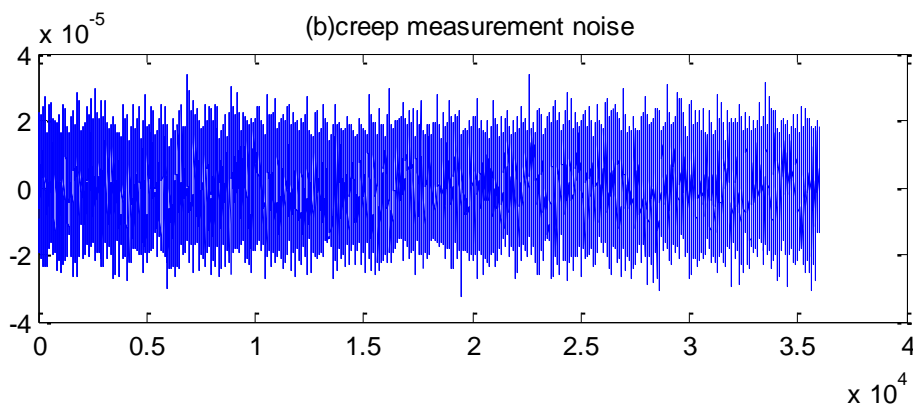


Figure 5 : Creepmeasurement noise

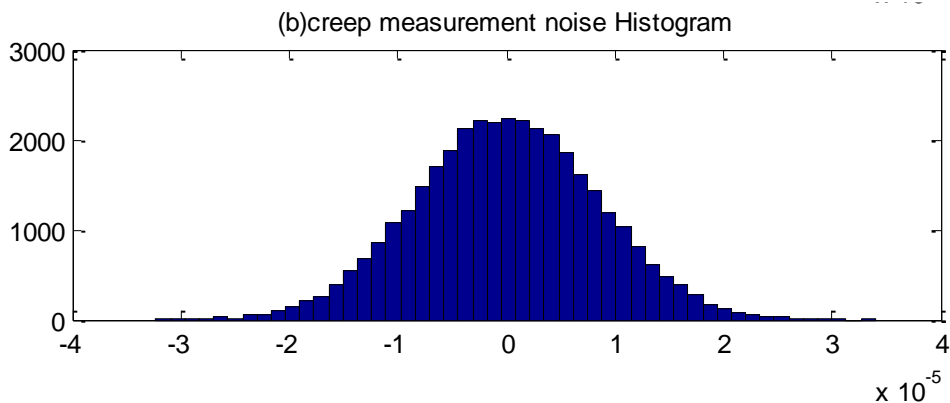


Figure 6 : Creepmeasurement noise histogram

6 Conclusion

The aim of this research work was the prediction of the creep behavior of the Cameroonian wood species "*Millettia Laurentii*" by the means of the discrete Kalman filter. The numerical results obtained through the Matlab software and exposed here are clearly stating that: the variance of the estimation error is minimal, the estimate and the real state have the same mean value confirming the idea that our estimator is not biased. This work is a pure demonstration of how the Kalman filter behaves when applied to creep behavior of wood and of polymeric materials in general. The authors [23-27] in their research works modeled the creep behavior of raphiavinifera and hard wood by rheological and empirical models. From a simple comparison between their results and ours, there is no doubt that the Kalman filter is more precise and offers more confidence because one can predict the correct state of a dynamic system from an initial doubtful or corrupted information.

7 References

- [1] Claire, B. (2001) Etude des propriétés mécaniques et du retrait au séchage du bois à l'échelle de la paroi cellulaire : essai de compréhension du comportement macroscopique paradoxal du bois de tension à couche gélatineuse (*Thèse de Doctorat*). Université de Montpellier, France.

- [2] Claire, B. & Thibaut, B. (2001) Shrinkage of gelatinous layer of poplar and beech tension wood. *IAWA Journal*, 22:2, 121-131.
- [3] Triboulot, P. & Duchanois, G. (1996) Pour une approche novatrice du matériau bois. *Revue technique luxembourgeoise*, no 3, France.
- [4] Triboulot, P. & Triboulot, M. C. (2000) Bois et matériaux dérivés. Refonte C 925. Techniques de l'ingénieur-construction. France.
- [5] Giannopoulos, I. (2009) Creep and creep-rupture behaviour of aramid fibres. University of Cambridge, United Kingdom.
- [6] Giannopoulos, I. P. & Burgoyne C. J. (2011) Prediction of the long term behaviour of high modulus fibres using the stepped isostress method (SSM). *Journal of matter science*.
- [7] Craig, J. & Mandel, J. (2006) A two stage ensemble Kalman filter for smooth data assimilation, *Journal of data science* 4: 21-37.
- [8] Dieter, G. E. (1988) Mechanical metallurgy. McGraw-Hill book company, Pp 152-160.
- [9] Zhao, Y., Bo Liang, B. & Iwnicki, S. (2014) Friction coefficient estimation using an unscented Kalman filter, *International Journal of Vehicle Mechanics and Mobility* 52(1): 53-70.
- [10] Evensen, G. (2003) The ensemble Kalman filter, Theoretical formulation and practical implementation, *Ocean Dynamics* 53: 343-367.
- [11] Brown, R. G. & Hwang, P. Y. C. (1992) Introduction to random signals and applied Kalman filtering. Second edition, John Wiley & Sons, Inc. Pp 4-5
- [12] Welch, G. & Bishop (2006) An introduction to the Kalman filter. TR 95-041, Department of computer science, University of North Carolina at Chapel Hill, Chapel Hill, NC 27599-3175, Pp 3-6.
- [13] Martin, V. (2004) Methods of navigation. *Lecture notes*, department of surveying of Helsinki University of technology (http://www.hut.fi/mvermeer/nav_en.pdf).
- [14] Matthew, B. R., Roger, A. S. & Keaton, H. (2017). A Kalman filtering tutorial for undergraduate students. *International Journal of Computer Science & Engineering Survey (IJCSSES)*, 8(1), 1-18.
- [15] Valliyappan, D. (2009) Constitutive behavior of a twaron fabric/natural rubber composite: experiments and modeling. Texas A&M University, USA.
- [16] Alger, M. (1997) Polymer Science Dictionary. Chapman and Hall, London, United Kingdom.
- [17] Brinson, H. F. & Brinson, L.C. (2008) Polymer Engineering Science and Viscoelasticity: An Introduction. Springer, New York.
- [18] Cheng, M. & Chen, W. (2006) Modeling transverse behavior of Kevlar® KM2 single fibers with deformation-induced damage. *International Journal of Damage Mechanics* 15, 121-132.
- [19] Guerira, B. (2016) Contribution dans l'exploration des phénomènes viscoélastiques non linéaires decomposites thermoplastiques. (*Thèse de Doctorat*). Université Mohamed Khider-Biskra, Algérie.
- [20] Ke-Chang, H. & Jyh-Horng, W. (2018) Effect of SiO₂ content on the extended creep behavior of SiO₂-based wood inorganic composites derived via the sol-gel process using the stepped isostress method. *Polymers*, 10(409).

- [21] Ratchada, S. and Raffaella, D.V. (2011) A Mathematical Model for Creep, Relaxation and Strain Stiffening in Parallel-Fibered Collagenous Tissues. *Journal of Medical Engineering and Physics*, 33, 1056-1063.
- [22] Kleinbauer, R. (2003) Kalman filtering implementation with matlab. *study report in the field of study geodesy and geoinformatics*, Helsinki, Finland.
- [23] Talla, P. K. (2008) Contribution à l'analyse mécanique de *Raphia Vinifera L. Arecacea (Thèse de Doctorat)*. Université de Dschang, Cameroun.
- [24] Talla, P. K., Mabekou, J. S., Fogué, M., Fomethé, A., Foadieng, E. & Foudjet, A. (2010) Non-linear creep behaviour of *Raphia Vinifera L. Arecacea* under flexural load. *International journal of mechanics and solids*, 5, 151-172.
- [25] Talla, P. K., Pelap, F. B., Fogué, M., Fomethé, A., Bawe, G. N., Foadieng, E. & Foudjet, A. (2007) Non-linear creep behaviour of *Raphia Vinifera L. Arecacea*. *International Journal of mechanics and solids*, 2, 1-11.
- [26] Talla, P.K., Foadieng, E., Fouotsa, W.C.M., Fogue, M., Bishweka, S., Ngarguededjim K.E., Alabeweh, F.S. and Foudjet, A. (2015) A Contribution to the Study of Entandrophragma *Cylindricum Sprague* and *Lovoa Trichilioides Harms* Long Term behavior. *Revue scientifique et Technique Foret et Environnement du Bassin du Congo*, X, 10-21.
- [27] Atchounga, P.K., Kamdjo, G., Foadieng, E. and Talla, P.K. (2017) Creep Modelling of a Material by Non-Linear Modified Schapery's Viscoelastic Model. *World Journal of Engineering and Technology*, 5, 754-764.